Extremophiles (2014) 18:311–329
DOI 10.1007/s00792-013-0617-6

ORIGINAL PAPER

Characterization of bacterial diversity associated with microbial mats, gypsum evaporites and carbonate microbialites in thalassic wetlands: Tebenquiche and La Brava, Salar de Atacama, Chile

M. E. Farías · M. Contreras · M. C. Rasuk · D. Kurth · M. R. Flores · D. G. Poiré · F. Novoa · P. T. Visscher

Received: 13 June 2013 / Accepted: 5 December 2013 / Published online: 18 January 2014

Abstract In this paper, we report the presence of sedimentary microbial ecosystems in wetlands of the Salar de Atacama. These laminated systems, which bind, trap and precipitate mineral include: microbial mats at Laguna Tebenquiche and Laguna La Brava, gypsum domes at Tebenquiche and carbonate microbialites at La Brava. Microbial diversity and key biogeochemical characteristics of both lakes (La Brava and Tebenquiche) and their various microbial ecosystems (non-lithifying mats, flat and domal microbialites) were determined. The composition and abundance of minerals ranged from trapped and bound halite in organic-rich non-lithifying mats to aragonite-dominated lithified flat microbialites and gypsum in lithified domal structures. Pyrosequencing of the V4 region of the 16s rDNA gene showed that Proteobacteria comprised a major phylum in all of the microbial ecosystems studied, with a marked lower abundance in the non-lithifying mats. A higher proportion of Bacteroidetes was present in Tebenquiche sediments compared to La Brava samples. The concentration of pigments, particularly that of Chlorophyll *a*, was higher in the Tebenquiche than in La Brava. Pigments typically associated with anoxygenic phototrophic bacteria were present in lower amounts. Organic-rich, non-lithifying microbial mats frequently formed snake-like, bulbous structures due to gas accumulation underneath the mat. We hypothesize that the lithified microbialites might have developed from these snake-like microbial mats following mineral precipitation in the surface layer, producing domes with endoevaporitic communities in Tebenquiche and carbonate platforms in La Brava. Whereas the potential role of microbes in carbonate platforms is well established, the contribution of endoevaporitic microbes to formation of gypsum domes needs further investigation.

Keywords Hypersaline lakes · Microbial mats · Microbialites · Atacama

Communicated by A. Oren.

M. E. Farías (✉) · M. C. Rasuk · D. Kurth · M. R. Flores
Laboratorio de Investigaciones Microbiológicas de Lagunas Andinas (LIMLA), Planta Piloto de Procesos Industriales Microbiológicos (PROIMI), CCT, CONICET, Tucumán, Argentina
e-mail: mefarias2001@yahoo.com.ar; mefarias@proimi.org.ar
URL: http://www.limla.com.ar

M. Contreras · F. Novoa
Centro de Ecología Aplicada (CEA), Suecia 3304, Ñuñoa, 2-2741872 Santiago, Chile

D. G. Poiré
Centro de Investigaciones Geológicas, Universidad Nacional de La Plata-Conicet, calle 1 no 644, 1900 La Plata, Argentina

P. T. Visscher
Center for Integrative, Geosciences University of Connecticut, 354 Mansfield Road, Storrs, CT 06269, USA

P. T. Visscher
Australian Centre for Astrobiology, University of New South Wales, Sydney, NSW 2052, Australia

Introduction

Over the past decades, the role of microorganisms in geological processes, particularly in microbially induced mineral precipitation (also referred to as organomineralization) has gained much attention in sedimentological and geomicrobiological literature (Reid et al. 2000; Dupraz et al. 2004, 2009; Dupraz and Visscher 2005; Glunk et al. 2011). From the Eoarchaean (4–3.6 Gy bp), microbes have played

a crucial role in the geochemical processes that form our planet's sedimentary record (Knoll and Golubic 1992; Gerdes 2007; Dupraz et al. 2009): in laminated organosedimentary structures or microbial mats, they stabilize sediments (Paterson 1994), mediate mineral precipitation or dissolution (Visscher and Stolz 2005), impact microfabric (Dupraz et al. 2009), influence the mineral composition and morphology (Braissant et al. 2004) and are capable of shaping the macrostructure of buildups (Burne and Moore 1987; Reid et al. 2000). In the organomineralization process, where microbes alter the geochemistry of their immediate microenvironment through metabolic activities and induce or influence mineral precipitation (Dupraz et al. 2009), mineral fabrics can be altered (Beveridge 1981; Cody and Cody 1989; Gerdes et al. 1994; Ludwig 2004; Douglas 2005; Ali-Bik et al. 2011). Furthermore, microorganisms typically have anionic cell surfaces that act as effective nucleating agents for mineral precipitation by scavenging metal ions from their environment (Beveridge 1981; Douglas 2005; Dupraz and Visscher 2005). Exopolymeric substances (EPS), produced by a variety of mat organisms (Decho 2000; Gallagher et al. 2010) consist of an organic matrix with anionic functional groups capable of binding metal ions like Ca^{2+} (Braissant et al. 2007). When microbes degrade EPS, Ca^{2+} is liberated and carbonate minerals precipitate (Dupraz and Visscher 2005; Glunk et al. 2011). This organomineralization process can result in the lithification of microbial mats, thereby forming modern microbialites (Dupraz et al. 2009). In contrast to the organic-rich, non-lithifying mats that consist largely of biomass with sporadically bound and trapped particle inclusions, microbialites are organosedimentary deposits that have accreted as a result of benthic microbial trapping and binding of sediment and, in addition, also mineral precipitation (Burne and Moore 1987). The microbialites in this study are actively forming at the surface, undergoing early diagenesis at the subsurface, and are therefore referred to as modern microbialites (Dupraz et al. 2011). Evidence from abundant fossil microbialites in the rock record suggests that microorganisms have engaged in organomineralization for most of Earth's history (Riding 2011).

Most investigations of microbial-induced organomineralization focus on carbonates: calcite and/or aragonite (Arp et al. 1999a, b; Reid et al. 2000, 2003; Reitner et al. 2005; Jahnert and Collins 2013), magnesium calcite including dolomite (Vasconcelos and McKenzie 1997; Glunk et al. 2011) and magnesite (Thompson and Ferris 1990; Sanz Montero and Rodríguez Aranda 2008). Microbial mats associated with halite and gypsum crusts are commonly referred to as endoevaporitic mats (Rothschild et al. 1994). They form through physicochemical mineral precipitation due to evaporation producing crusts and "stromatolite-like" domal structures (Babel 2004; Stivaletta et al. 2010). These laminated microbial endolithic domal structures are often referred to as endoevaporites (Rothschild et al. 1994; Spear et al. 2003; Canfield et al. 2004; Sahl et al. 2008). The exact role of microbes in the formation of these gypsum domes is not well established. Some of the physical properties of gypsum, such as translucency and hygroscopy, are favorable for the development of endoevaporitic microbial mats (Rothschild et al. 1994; Oren et al. 1995; Stivaletta and Barbieri 2009). Despite the abundance of extant and extinct ecosystems where microbes are associated with gypsum (Babel 2004; Oren et al. 1995; Vogel et al. 2009), few studies have focused on the role of microorganisms in $CaSO_4$ precipitation.

One of the Earth's largest evaporitic basins, Salar de Atacama, located in the Chilean central Andes, is comprised of a large number of closed basins in which *salares* form. These *salares* are saline lakes (locally referred to as "*lagunas*") at the edge of which evaporitic crusts form (Stoertz and Ericksen 1974; Risacher et al. 2003).

In this study, we compare two *lagunas* in Salar de Atacama in which a variety of non-lithifying microbial mats and microbialites, including calcium carbonate platforms and endoevaporitic gypsum domes, form. We provide a description of these ecosystems, including the setting, the composition of their mineral phase and the microbial diversity.

Materials and methods

Site description

The Salar de Atacama depression is a distinct geomorphologic structure in northern Chile (Risacher et al. 2003) and is the oldest and the largest evaporitic basin in that country. It is a tectonic intramontane basin filled with Tertiary to Quaternary clastic and evaporitic sediments of continental origin. The Salar's hydrogeological setting is quite complex, receiving both surface and groundwater inputs predominantly from the east (Bevacqua 1992). The main water input is through leaching and direct contributions of Tertiary and Quaternary volcanic material. In the lowest region of Atacama basin, groundwater surfaces, forming a series of lakes include: Laguna de Piedra, Laguna Tebenquiche, Chaxas, Burro Muerto and La Brava (Alonso and Risacher 1996). The environmental conditions of these lakes are characterized by (1) high solar radiation due to a lower barometric pressure at high altitude, and consequently decreased absorption of solar radiation (Cabrera and Pizarro 1994), (2) extreme diel temperature fluctuations typical of desert environments, (3) net evaporation producing hypersaline water and (4) high arsenic concentrations in the water due to volcanic events (Lara

et al. 2012). All these conditions contribute to an environment that selects for microbial extremophiles.

Previous microbiological studies in Salar de Atacama have focused on the diversity (Dorador et al. 2009) and aresenic resistance (Lara et al. 2012) of water and sediments in Laguna Tebenquiche, Burro Muerto, and Chaxas. To date, no geomicrobial investigations that include diversity studies of the endoevaporitic gypsum domes in La Brava and Tebenquiche have been published.

The Salar de Atacama comprises two main units: a core and a marginal zone. The core (1,100 km^2 and 900 m thick) consists of a porous halide (90 %) impregnated with a sodium chloride brine rich in lithium (Li), potassium (K), magnesium (Mg) and boron (B) occupying the interstices of the halide. The marginal zone of the Salar consists of thin saline sediments that are rich in sulfates, especially gypsum (Bevacqua 1992; Alonso and Risacher 1996). There are two types of brines in the Salar de Atacama: type Na–Ca–(Mg)–Cl ("calcium" brines) and other types of Na–(Mg)–SO_4–Cl ("sulfate" brines) (Alonso and Risacher 1996). Tebenquiche is located closer to the core and La Brava is in the marginal zone.

Sample site and sample collection

A variety of microbial mats associated with and water samples from the respective sites were collected during two field campaigns in March and November of 2012. Tebenquiche samples included non-lithifying microbial mats (TM) and gypsum domes (TD) and La Brava samples included non-lithifying mats (BM) and microbialites (BMI). At the time of sampling, the microbial mats (TM, BM) were submersed in few cm of water and TD and BMI were found at 15–30 cm depth in the lake.

Samples were taken in triplicate from each sampling site: 2 cm^2 with an arbitrarily depth of 3 cm, which included several mat layers and at least the upper three layers (green, purple and dark) of the domes (TD) and microbialites (BMI). The triplicate samples were homogenized and aliquots were used for analyses of DNA, photopigments, organic matter content and mineralogy. For scanning electron microscopy (SEM) determination, samples were fixed over night at 4 °C in a Karnovsky fixative comprising formaldehyde (8 % v/v), glutaraldehyde (16 % v/v) and phosphate buffer (pH 7).

Samples for SEM and mineralogy of the mats and the microbialites as well as for water chemistry were stored in the dark at 4 °C and processed within 1–2 weeks. Samples for DNA extraction were frozen in liquid nitrogen, stored in the dark and further processed within a week. Microelectrode profiles were measured in situ during the November campaign (see below). Water samples were analyzed in situ for temperature and pH, and in the laboratory for dissolved oxygen, salinity, conductivity, chlorophyll, total P, NO_3^-, NO_2^-, dissolved Si, Ca, Mg and major ions (K^+, SO_4^{2-} and Na^+), according to the methodology described by Eaton et al. (2005). NH_4^+, orthophosphates and Total Organic Nitrogen (NOT) were analyzed using a Merck Nova 60Spectrocuant instrument. Loss on Ignition (LOI) analysis was used to determine the organic matter content (%OM) of sediment samples. The difference in weight of 5 g of sample before and after heating for 2 h at 450 °C was determined in order to calculate the amount of the OM. All analyses were carried out in triplicate.

Photosynthetically active radiation (PAR; 400–700 nm) was measured using a LiCor LI 250A light meter with a LiCor LI190 quantum sensor (LiCor Biosciences, Lincoln, NE, USA) and UV A-B (280–400 nm) measurements were made with a Solar Light CO. PMA 2100 radiometer (Solar Light Company, Inc., Glenside, PA, USA).

Microelectrode measurements

Oxygen and sulfide concentrations in mats and microbialites were determined in situ at both La Brava (BM and BMI) and Laguna Tebenquiche sites (TM and TD). Measurements were taken during the middle of the day (light intensity of PAR was 1,850–2,550 $\mu E\ m^{-2}\ s^{-1}$). Clark-type oxygen and amperometric sulfide needle electrodes both with built-in guard cathode and reference electrodes were connected to a portable picoammeter (Unisense PA 2000, Arhus, Denmark). The sensors were deployed in 200–250 μm depth increments using a manual micromanipulator (National Aperture, New Hampshire). Three to five replicate profiles covering the upper 10–15 mm of each mat were measured and profiles constructed using calibration curves determined before and after the measurements. Microbial mats and microbialites display slight variations in sedimentary features (e.g., thickness of the mineral crust, depth and thickness of the cyanobacterial layer, etc.) and therefore representative profiles were chosen for publication. The average depth of O_2 penetration and standard deviation of replicate profiles was calculated and similarly, the average concentration at the O_2 maximum and its corresponding standard deviation was also determined. The oxygen concentration was corrected for salinity and temperature (Sherwood et al. 1991) and values determined for an atmospheric pressure of 1 bar. Corrections for altitude were made using $p = p_0.e^{-(h/h_0)}$. For $h = 2{,}300$ m, which is the approximate altitude of the Salar de Atacama, using a scale height h_0 of the Earth's atmosphere of ca. 7,000 m, an atmospheric pressure p_0 at sea level of 1 bar, the air pressure p is 0.719 bar. The needles were able to penetrate the submersed halide and gypsum crusts of up to 8–10 mm in thickness. Light

measurements of PAR were made throughout the duration of the measurements as described above.

Mineralogical analysis using XRD and SEM–EDAX

Mineral composition of the non-lithifying mats, gypsum domes and microbialites was obtained by X-ray diffraction (XRD) analyses, which were carried out on finely ground sample material (<20 μm), measured with a PANalytical X′Pert PRO diffractometer, with Cu lamp ($k\alpha = 1.5403$ Å) operated at 40 mÅ and 40 kV at the Centro de Investigaciones Geológicas (La Plata, Argentina).

Light and scanning electron microscopy

Macro- and micro-scale observations were made using an Olympus SZX12 stereoscope and an Olympus BX60 microscope with a C-2000Z digital camera, respectively. For scanning electron microscopy (SEM), samples were fixed overnight at 4 °C in a Karnovsky's fixative comprised of formaldehyde (8 % v/v), glutaraldehyde (16 % v/v), and phosphate buffer (pH 7). The samples were washed three times with phosphate buffer and $CaCl_2$ for 10 min and fixed with 2 % v/v osmium tetroxide overnight. The samples were washed twice with ethanol 30 % v/v during 10 min, dried at critical point and sputtered with gold. Specimens were observed under vacuum using a Zeiss Supra 55VP (Carl Zeiss NTS GmbH, Germany) scanning electron microscope. Elemental analyses were done using energy dispersive X-ray spectroscopy (EDAX) using an INCA Penta FET-X3 EDS detector (Oxford, UK) and spectra were analyzed using the INCA Energy software interface.

Pigment identification by HPLC

Pigment analysis was done by high-performance liquid chromatography (HPLC) (Borrego and Garcia-Gil 1994). Samples (1.5 g of mats, lithified domes or microbialites) were frozen in liquid nitrogen, ground in a mortar and subsequently freeze-dried. Equal subsamples (0.2 g) of these freeze-dried samples were mixed with 2 ml of 100 % methanol and dark incubated overnight at −20 °C. Methanol extracts were centrifuged at 8,000 *g* for 10 min at 4 °C and the supernatants were filtered through 0.2-μm pore-diameter syringe filters before the HPLC analysis.

HPLC analysis was performed to determine the numbers and abundances of unique pigments. The HPLC system consisted of 2 pumps (Waters, model 510), a syringe loading injector (Rheodyne 7125) fitted with 200 μl loop (Rheodyne 7025), and a on-line detection by diode array-based spectroscopy between 250 and 800 nm (Waters 996) coupled to a computer equipped with the Empower 2007 Chromatography Manager software (Waters-Millipore), allowing for the detection of pigments spectra. The column used was 100 × 4.6 mm Kinetex C-18 (3 μm silica particle size) protected by an Ultra In-Line Krudkatcher filter (Phenomenex).

Pigments were identified by comparing the peak retention times and the corresponding absorption spectra against standards available in the laboratory or, when not available, against data in the LipidBank database (http://www.lipidbank.jp). Pigment abundance was quantified based on the peak areas in the chromatograms measured at an absorption wavelength of 435 nm. Peak delimitation and area integration were carried out automatically by the instrument's software. Due to the lack of standards for most of the pigments that were detected, their peak areas were normalized to the highest area of known peak(s). Since all samples were collected and analyzed in the same way, the relative pigment abundances can be compared directly in all samples. In addition, Chlorophyll *a*, Beta-carotene, Lycopene, Diatoxanthin, Lutein, Canthaxanthin and Astaxanthin were identified and quantified using standards from DHI, Denmark. This was done only in the Tebenquiche samples as none of these pigments were detected in the La Brava samples.

DNA extraction

Total genomic DNA was obtained from subsamples taken as described above. Initial attempts using 0.2 g of material treated with the Power Biofilm DNA Isolation Kit (MO BIO Laboratories, inc.) were not successful for the microbialite (hard) samples. Thus, the method described by López-López et al. (2010) was used for all samples with minor modifications. In brief, we started with 10 g of material, and cells were separated from minerals and exopolymeric organic matrix by repeated washing in phosphate-buffered saline (PBS) with gentle shaking for 2 h, recovered by centrifugation and stored at −20 °C until extraction. For DNA extraction, cells were resuspended in 2 ml extraction buffer [100 mM Tris–HCl pH 8, 20 mM EDTA, 1.4 M NaCl, 2 % CTAB (hexadecyltrimethylammonium bromide 99 %)] and lysed in two steps. First, three freeze–thaw cycles of 15 min were carried out. Then, treatments with proteinase K, lysozyme and SDS 10 % were used to ensure complete lysis. DNA was purified from lysates with phenol:chloroform:isoamylalcohol 25:24:1 and ethanol precipitated.

PCR and pyrosequencing

The V4 hypervariable region of the Bacterial 16s rRNA gene was amplified using the Ribosomal Database Project (RDP)-suggested universal primers (http://pyro.cme.msu.

edu/pyro/help.jsp) that contain the Roche 454 sequencing A and B adaptors and a 10 nucleotide "multiple identifier" (MID). Five independent PCRs were performed to reduce bias. The PCR mixture (final volume 25 µl) contained 2.5 µl FastStart High Fidelity 10× Reaction Buffer (Roche Applied Science, Mannheim, Germany), 20 ng of template DNA, 0.4 µM of each primer, and 1.25 U FastStart High Fidelity Enzyme Blend (Roche Applied Science), and 0.2 mM dNTPs. The PCR conditions were 95 °C for 5 min for initial denaturalization, followed by 95 °C for 45 s, 57 °C for 45 s, 72 °C for 60 s in 30 cycles, and a final elongation step at 72 °C for 4 min. Two negative control reactions containing all components except for the template were performed. The five reactions' products were pooled and purified using AMPure beads XP. Quantification of the purified PCR product was performed using the Quant-IT Pico Green dsDNA Kit (Invitrogen Molecular Probes Inc, Oregon, USA).

Purified PCR product was sequenced on a Genome Sequencer FLX (Roche Applied Science) using Titanium Chemistry according to the manufacturer's instructions. Analyses were performed at INDEAR (Argentina) genome sequencing facility. 11,139 filtered sequences with an average length of 248 bp were obtained from four samples used in this study. Filter parameters were set to reject reads that had mean quality score <25, maximum homopolymer run >6, number of primer mismatches >0, and read length <200 bp or >1,000 bp. Sequences were deposited as FASTAQ in the NCBI Sequence Read Archive (SRA) under the following accession number SRA061755.

Taxonomy-based and alpha diversity analysis

Diversity of the microbial community was assessed by analyzing the sequences of the V4 hyper variable region of Bacterial 16s rRNA using the QIIME software package v.1.5.0 (Caporaso et al. 2010). Sequences were clustered into OTUs using UCLUST at the 97 % similarity level using the most abundant sequence as the representative sequence for each OTU. A table was compiled of the number of sequences per OTU. Each representative OTU sequence was characterized taxonomically with the RDP classifier using the Ribosomal Database Project (RDP) database included in QIIME v1.5.0 software using a bootstrap confidence of 50 %. Other public datasets including Socompa stromatolite, SRP007748 (Farías et al. 2013), Atacama hyper-arid soils, SRA030747 (Neilson et al. 2012), Yellowstone stromatolites (http://inside.mines.edu/~jspear/resources.html) (Pepe-Ranney et al. 2012), Highborne Cay stromatolites, Bahamas (GenBank accession numbers FJ911975–FJ912833) (Baumgartner et al. 2009a), Highborne Cay thrombolites, SRX030166 (Mobberley et al. 2012), and a Guerrero Negro microbial mat, (GenBank accession numbers DQ329539–DQ331020 and DQ397339–DQ397511) (Ley et al. 2006) were analyzed using same procedures for comparative analysis.

OTU tables were subsampled using 10 replicates for each sampling effort at increasing intervals of 350 sequences and alpha diversity indices were calculated on each subsample of the rarefaction curve and on the complete OTU table (including all sequences) using QIIME. Alpha diversity metrics calculated included observed species, CHAO1, Shannon, Simpson, Equitability and Dominance indices.

Samples from this work were compared with the publicly accessible datasets listed above. For this comparison, an UPGMA tree was constructed in QIIME, based on Bray Curtis distances between samples measured from the relative abundances at the phylum level.

Results

Physicochemical characteristics

Water temperature in Tebenquiche reached 21.5 °C in March and 31.0 °C in November, and correspondingly, 24.6 and 30.1 °C in La Brava (Table 1). Based on pH measurements (7.4–8.6 and 7.8–8.2 for Tebenquiche and La Brava, respectively), both systems can be classified as moderately alkaline (Hounslow 1995). Saline and hypersaline conditions were determined (38–150 g/L brine). Relative ions concentration were similar in both systems chloride > sodium > sulfate > potassium > magnesium > calcium. Incident UVA-B radiation measured in both environments showed that maximal UV-AB reached 57.9 W m^{-2} at noon in La Brava, while in Tebenquiche the maximal UV-AB reached 53.4 W m^{-2} at noon.

Distribution and macromorphology of microbial mats, domes and microbialites

Tebenquiche and La Brava lakes display a characteristic salinity gradient that results from ground and/or superficial water input and evaporation (Risacher et al. 2003). Along the salinity gradients, different microbial ecosystems developed: organic-rich, non-lithifying microbial mats were found along the shoreline at low salinity (62 g/L) at Tebenquiche and, with increasing salinity (116 g/L), the amount of mineral precipitation and hence lithification increased as well. At La Brava, the opposite situation was observed: mats were present near the shore at a higher salinity (119 g/L) and microbialites (i.e., intermediate and fully lithified, hard mats; Fig. 2) were found submerged in the lake where a lower salinity (72 g/L) prevailed. The

Table 1 Physicochemical parameters measured in the water column of Laguna Brava and Laguna Tebenquiche, Salar de Atacama

	Units	La Brava	Tebenquiche
Temperature	°C	24.6	21.5
pH	–	7.9	8.6
Physico-chemical			
Dissolved oxygen	mg/L	3.75	2.20
Salinity	g/L	70.8	102.0
Conductivity	mS/cm	107.3	138.7
Chlorophyll *a*	mg/L	–	2.875
Total Phosphorus	mg/L	1.70	1.41
Orthophosphate	mg/L	2.49	0.74
Ammonium	mg/L	0.24	–
Nutrients			
Total organic nitrogen	mg/L	0.92	0.513
Nitrate	mg/L	–	2.6
Nitrite	mg/L	–	0.0002
Dissolved Silica	mg/L	32	96
Calcium	mg/L	812	1,164
Magnesium	mg/L	2,568	2,705
Major ions			
Potassium	mg/L	6,072	5,121
Sulfate	mg/L	565	20,388
Sodium	mg/L	17,810	40,640
Chloride	mg/L	43,057	64,290
Hardness	mg/L	12,603	14,042
Organic matter	%	–	7.5
Total organic carbon	mg/L	–	44.5
Other environmental parameters			
Total sulfur	mg/L	–	<0.2
Dissolved sulfur	mg/L	–	6,876
Arsenic	mg/L	–	2.3

increasing mineral incorporation in mats was confirmed by the increased mechanical resistance during deployment of microelectrodes. In the submerged zone at high salinity, extensive areas of hard domes thrive (Fig. 1b, c). The soft microbial mats have a variety of macroscopic morphologies including small *domes,* and *cerebroid, snake* and *globular* morphologies (Fig. 2a–e) (compare with Dupraz et al. 2009; Glunk et al. 2011; Jahnert and Collins 2011). In some areas, bulbous mats accumulate gas at the subsurface as seen in cross section of Fig. 2b. The submerged non-lithified mats have a typical pink appearance (Fig. 2a, d), however, when exposed to the air, a white evaporitic crust covers the surface (Fig. 2b). At the highest observed salinity (117 g/L), a hard domal structure forms (Fig. 1b): this area of higher salinity (conductivity) supports formation of domal structures (Figs. 1b, c, 2g, h). In La Brava, the microbialites grow upward until they reach the water/air interface when they continue to spread laterally and form platforms (Figs. 1c, 2i). These microbialites display a typical sequence of (from top to bottom) white, green, purple and dark colored layers.

Mineralogy XRD–EDAX–SEM and organic matter determination

XRD analyses revealed that Tebenquiche microbial mats comprised predominantly halite (42 %) with minor contributions of calcite (22 %), gypsum (22 %) and aragonite (12 %), and the domal evaporitic systems from Tebenquiche consisted entirely of gypsum; (Fig. 3a, b). In La Brava, the mineralogical analyses of the microbial mats revealed halite (82 %) as the major and aragonite (13 %) and calcite (7 %) as minor components (Fig. 3c). La Brava microbialites consisted exclusively of aragonite ($CaCO_3$) (Fig. 3d).

Scanning electron microscopy revealed that both mats and domes contained microbes that were associated with minerals: cyanobacteria, diatoms, and other microorganisms were part of the lithified structures. SEM and EDAX confirmed the mineralogical results obtained by XRD (See above; Fig. 3): both La Brava and Tebenquiche microbial mats contained aragonite minerals (Fig. 4b), the domes in Tebenquiche comprised of gypsum only (Fig. 4e) and La Brava's microbialites contained aragonite (Fig. 4g). Cyanobacterial morphologies were found in mats and domes (Fig. 4a, d). Bacteria associated with aragonite or gypsum minerals were also observed (Fig. 4b, e). Diatoms were present in all samples (Fig. 4c, f).

XRD revealed that the elemental composition of the lithified layers was dominated by Si, and O in lithified organic part with minor contributions of Mg, Na and P (Fig. 4f, i) or S and Ca in gypsum domes (Fig. 4j) and the silica in diatoms frustules (Fig. 4h).

Organic matter content of the different mat systems showed a higher content in soft (non-lithifying) mats (34 ± 8.7 and 32 ± 11.3 % C for Brava and Tebenquiche, respectively) than in lithified counterparts (19 ± 5 % C in gypsum evaporites of Tebenquiche and 16 ± 6.8 % C in aragonitic microbialites in Brava).

Oxygen and sulfide profiles

Depth profiles showed typical subsurface O_2 maxima in all mat types that result from oxygenic photosynthesis (Fig. 5). Replicate profiles (not shown) displayed similar patterns, with slight differences in depth and magnitude of the oxygen peak (e.g., in Tebenquiche mats, the average depth of the O_2 peak was 1.79 mm with a standard deviation of 0.24, and a corresponding O_2 concentration average of 149 µM with a standard deviation of 20.7; in La

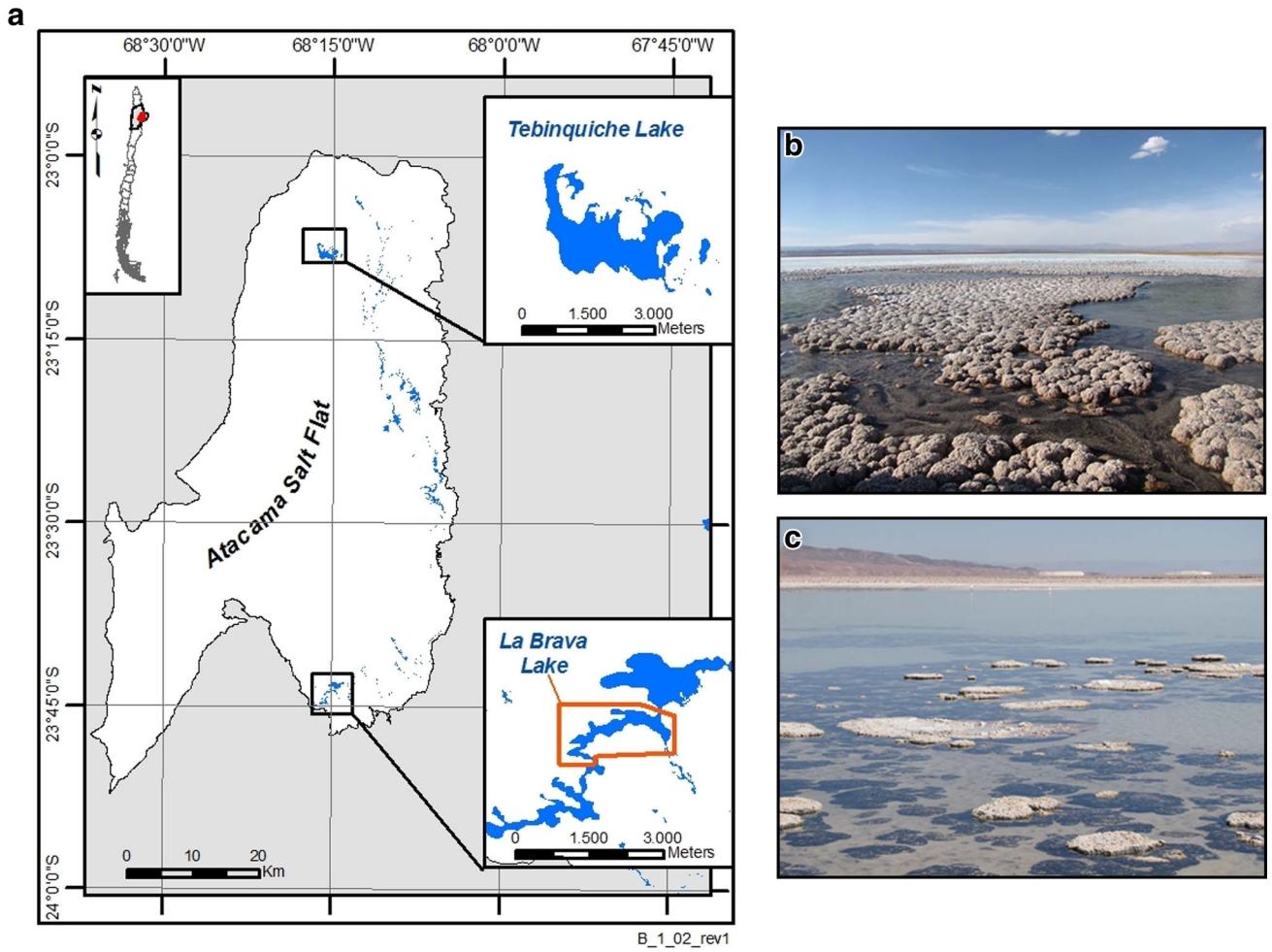

Fig. 1 **a** Location of the study area, which consists of a system of several lakes. The two lakes of this study are outlined in the two respective inserts. **b** Overview of Laguna Tebenquiche. **c** Overview of Laguna La Brava

Brava microbialites, average depth of the O_2 maximum was at 2.72 mm, standard deviation 0.33, with a corresponding average concentration of 225 μM, and standard deviation of 24.7). Due to differences in salinity and temperature in La Brava and Tebenquiche (i.e., resulting in different amounts of dissolved gas at saturation in both systems), a direct comparison of O_2 concentrations is not possible. Therefore, we use % of O_2 saturation below when comparing maximum O_2 concentrations in La Brava and Tebenquiche systems. The maximum values of oxygen saturation ranged from a peak value of ca. 130–150 % O_2 in the La Brava microbial mat and the Tebenquiche dome (underneath a gypsum crust of 5.5 mm thickness) to >200 % in the Tebenquiche (intermediate) mat and the La Brava microbialites (which had a carbonate crust of 1–2 mm). The mats with the lowest O_2 peak (Tebenquiche hard, La Brava soft mats) had little or no free sulfide at depth, whereas the mats with the highest O_2 peaks (Tebenquiche microbial mats and La Brava microbialites) displayed sulfide concentrations >100 μM at depth (Fig. 5).

Pigments analyses

Although the samples from Tebenquiche and La Brava had pigments in common, their pigment compositions markedly differed (Fig. 6; Table 2). The identity of the dominant pigments differed between the two sites (Table 2): Laguna Tebenquiche showed a higher amount of chlorophyll (Fig. 7c) and also higher diversity of pigments than Laguna Brava. For example, Lycopene, Chl *a*, Bchl *e*, Diadinoxanthin [and two unidentified pigments eluting at 20.73 and 23.37 min] were relatively abundant in Tebenquiche but not detected in La Brava. In contrast, La Brava samples were dominated by Echinenone, which was very minor in Tebenquiche mats and not detected in Tebenquiche domes. The diversity of pigments in the Tebenquiche mats was much higher than either in Tebenquiche

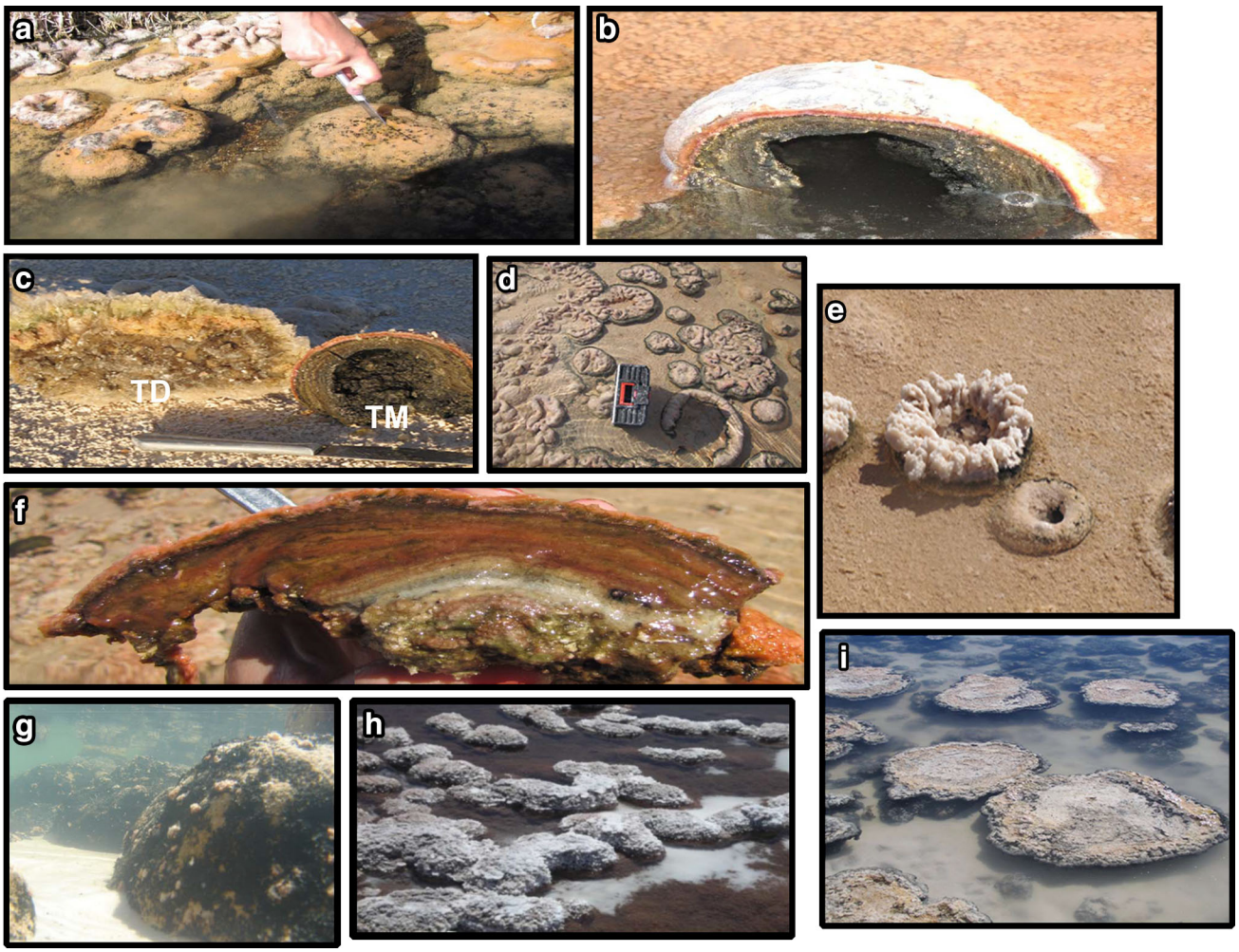

Fig. 2 Macroscopic images of mats and gypsum domes: **a** Microbial mats of Laguna Tebenquiche. **b** Cross section of a bulbous mat of Laguna Tebenquiche. **c** Cross section of dome (TD) and bulbous microbial mat (TM) of Laguna Tebenquiche. **d** Microbial mats of La Brava, showing the typical cauliflower and snake-like patterns. **e** Mineral crust overlaying an emerged microbial mat at La Brava. **f** Cross section of a microbial mat of La Brava. **g** Dome-shaped, submerged microbialites of La Brava. **h** Flattened domes of Laguna Tebenquiche. **i** Vertical view of La Brava microbialites

domes or in mats and microbialites from La Brava (Fig. 7). Lycopene derivatives and Fucoxanthin were common in all samples. Pigments such as Aloxanthin, Echinenone, Bacteriochlorophyll-*c* and a few unidentified pigments were common and relatively abundant in Tebenquiche mats and La Brava mats but were not detected in Tebenquiche domes and La Brava microbialites (Table 2).

Bacterial diversity

The bacterial 16S pyrotag sequences were classified at a similarity level of 0.97. At this level, richness and diversity metrics were statistically similar for most samples with the exception of TD (Table 3). In all of the samples, the collectors' curves did not reach an asymptote, suggesting that more OTUs are expected with a deeper sequencing effort (data not shown). The Tebenquiche gypsum domes (TD) formed a notable exception to the trend found for all the microbial mats and microbialite samples. In these samples, the number of observed OTUs was much lower, and correspondingly, the CHAO1 estimator of TD was also the lowest of the group. The diversity indices Dominance and Equitability show a similar pattern: the Dominance index, which suggests a higher representation of a limited number of OTUs, is the highest for TD and the Equitability index, which points to an uneven distribution among the taxa, is the highest for the TD sample. All other samples displayed similar low Dominance and high Equitability indices.

This dominance/equitability difference between TD and the rest of the samples is also clear when comparing the phyla that are present in all of the samples (Fig. 7). The gypsum dome appears less diverse than unlithified microbial mat samples at this level, with a lower number of phyla

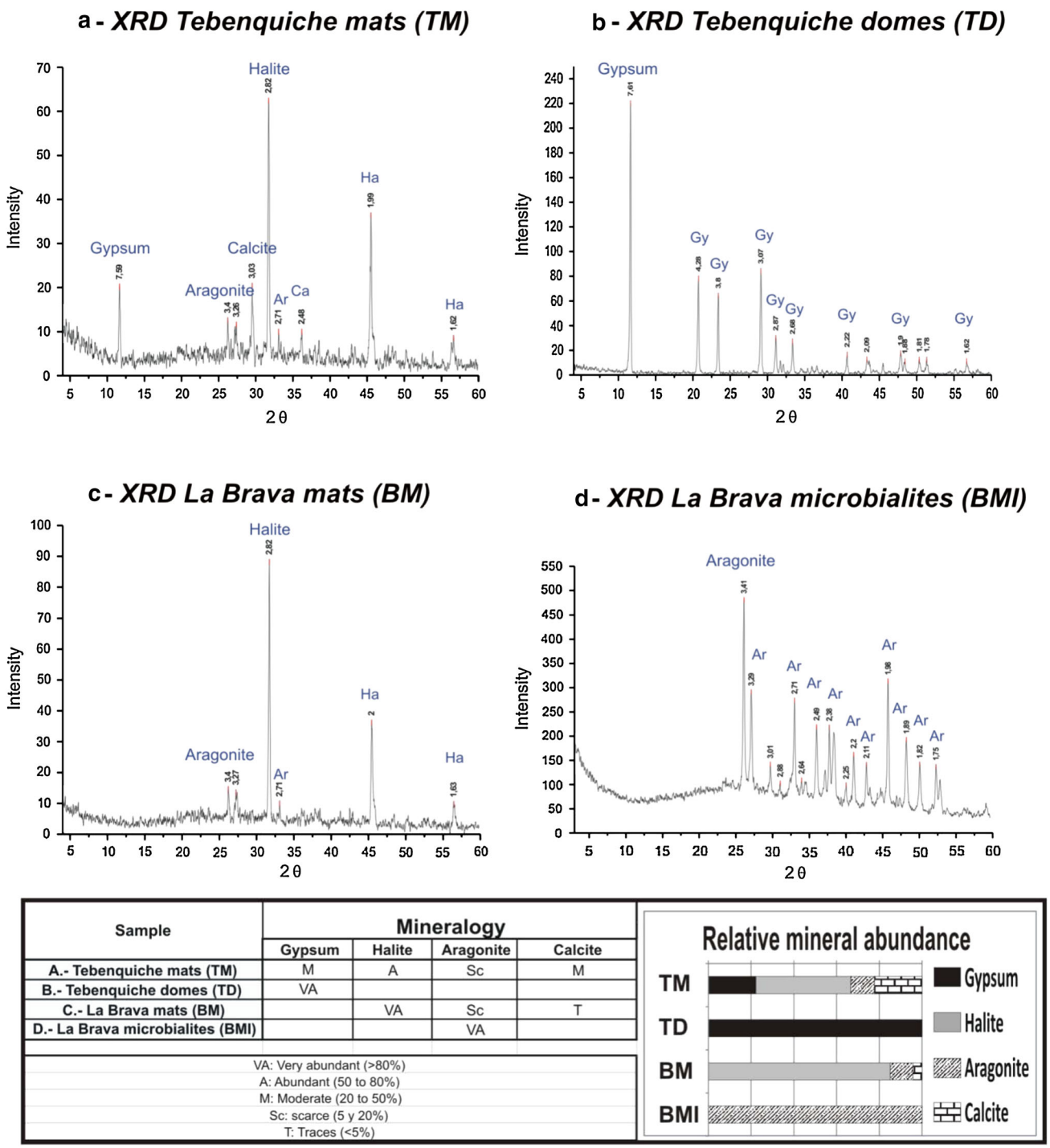

Sample	Mineralogy			
	Gypsum	Halite	Aragonite	Calcite
A.- Tebenquiche mats (TM)	M	A	Sc	M
B.- Tebenquiche domes (TD)	VA			
C.- La Brava mats (BM)		VA	Sc	T
D.- La Brava microbialites (BMI)			VA	

VA: Very abundant (>80%)
A: Abundant (50 to 80%)
M: Moderate (20 to 50%)
Sc: scarce (5 y 20%)
T: Traces (<5%)

Fig. 3 XRD spectra showing mineral composition of the mats and microbialites: **a** Tebenquiche microbial mats and **b** Tebenquiche domes. **c** La Brava microbial mats and **d** La Brava microbialites. Abundance of major minerals listed in table below the spectra

accounting for the majority of the sequences. In both TM and TD, Bacteroidetes were dominant, followed by Proteobacteria. These two groups (phyla) account for more than 90 % of the sequences in TD, which concurs with the low values of the diversity estimators discussed above. In comparison, these two phyla only account for 60 % in TM.

The lowest diversity of all the samples studied was found in TD, which was dominated by Bacteroidetes (49.1 %) and Proteobacteria (43.3 %) with the Alpha-Proteobacterial Rhodospirillales constituting the major fraction (37.2 % of total sequences). Moreover, within the two most abundant phyla, sequences showed very low

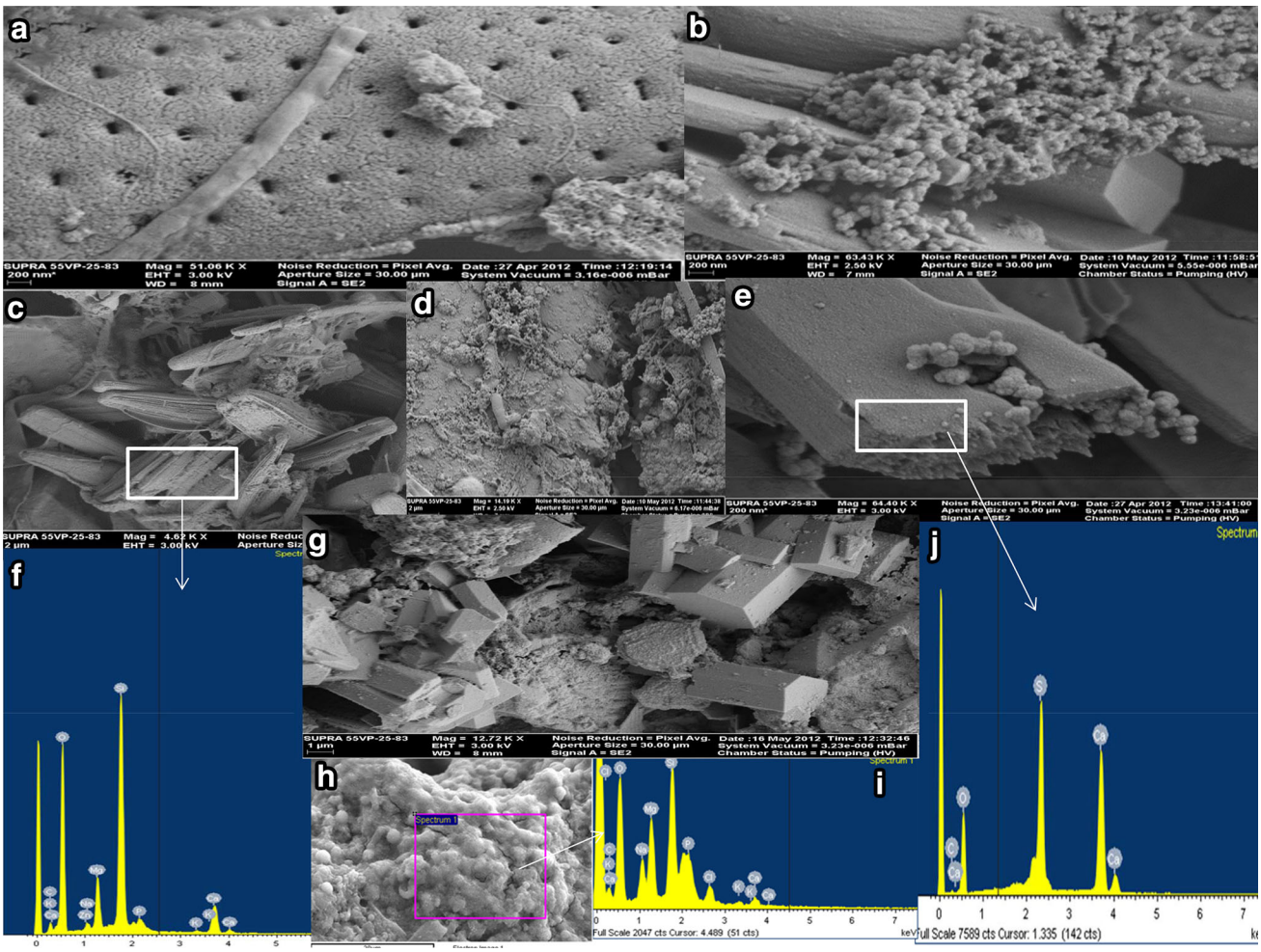

Fig. 4 Scanning Electron Microscopy (SEM; **a**–**e**, **g**, **h**) images and Energy Dispersive X-Ray analysis (EDAX; **f**, **i**, **j**) of studied microbial ecosystems: **a** Cyanobacteria overlaying diatom frustules in Tebenquiche microbial mats. **b** Aragonite minerals associated with bacteria in Tebenquiche microbial mats. **c** Diatoms from a Tebenquiche dome.**d** Cyanobacteria (*arrow*) from a Tebenquiche dome. **e** Bacteria on a gypsum crystal in a Tebenquiche dome. **f** EDAX of the diatom-dominated area (**c**) showing silica predominance. **g** Aragonite in a mat from La Brava. **h**–**i** Phosphate crystal covering microbial cells **j** EDAX from the gypsum crystal (**e**) showing abundance of sulfur and calcium

diversity: 99 % of the sequences classified as Bacteroidetes were affiliated with the Sphingobacteria class, Sphingobacteriales order, Rhodothermaceae family, and 86 % of the proteobacterial sequences were affiliated with the Alphaproteobacteria class. TM was also dominated by Bacteroidetes (38.9 %) and Proteobacteria (20.8 %), the latter with major contribution of the classes Alpha- and Deltaproteobacteria (5.7 and 7.5 % of total sequences, respectively). The Spirochaete phylum (8.7 %) was also well represented in the TM sample.

The dominant phylum in BMI comprised of Proteobacteria (41.8 %), with sequences distributed among the following classes and orders: Alphaproteobacteria with Rhodospirillales (7.6 %), Gammaproteobacteria with Chromatiales (10.5 %), and Deltaproteobacteria with *Syntrophobacter* and Desulfovibrionales (6 and 2.2 %, respectively). Other abundant phyla in BMI were Verrucomicrobia (11.8 %) and unclassified Bacteria (7.6 %). At BM Proteobacteria (22.3 %) was the most abundant phylum but not as abundant as in BMI. Within the BM Proteobacteria, classes and orders, respectively, of the Alphaproteobacteria with Rhodospirillales (7.5 %), and Deltaproteobacteria with *Syntrophobacter* (5.5 %) contributed the most. Thermi with Deinococcales (11.8 %), unclassified Bacteria (12.1 %) and Spirochaetes (10.4 %) were also abundant in BM. Comparison of the La Brava samples show that in BM eight phyla have >5 % of the total amount of sequences, while BMI only have four phyla with >5 % of the total sequences.

A noteworthy feature of all samples analyzed is that a significant number of sequences are marked as unclassified, stressing the singularity of these environments.

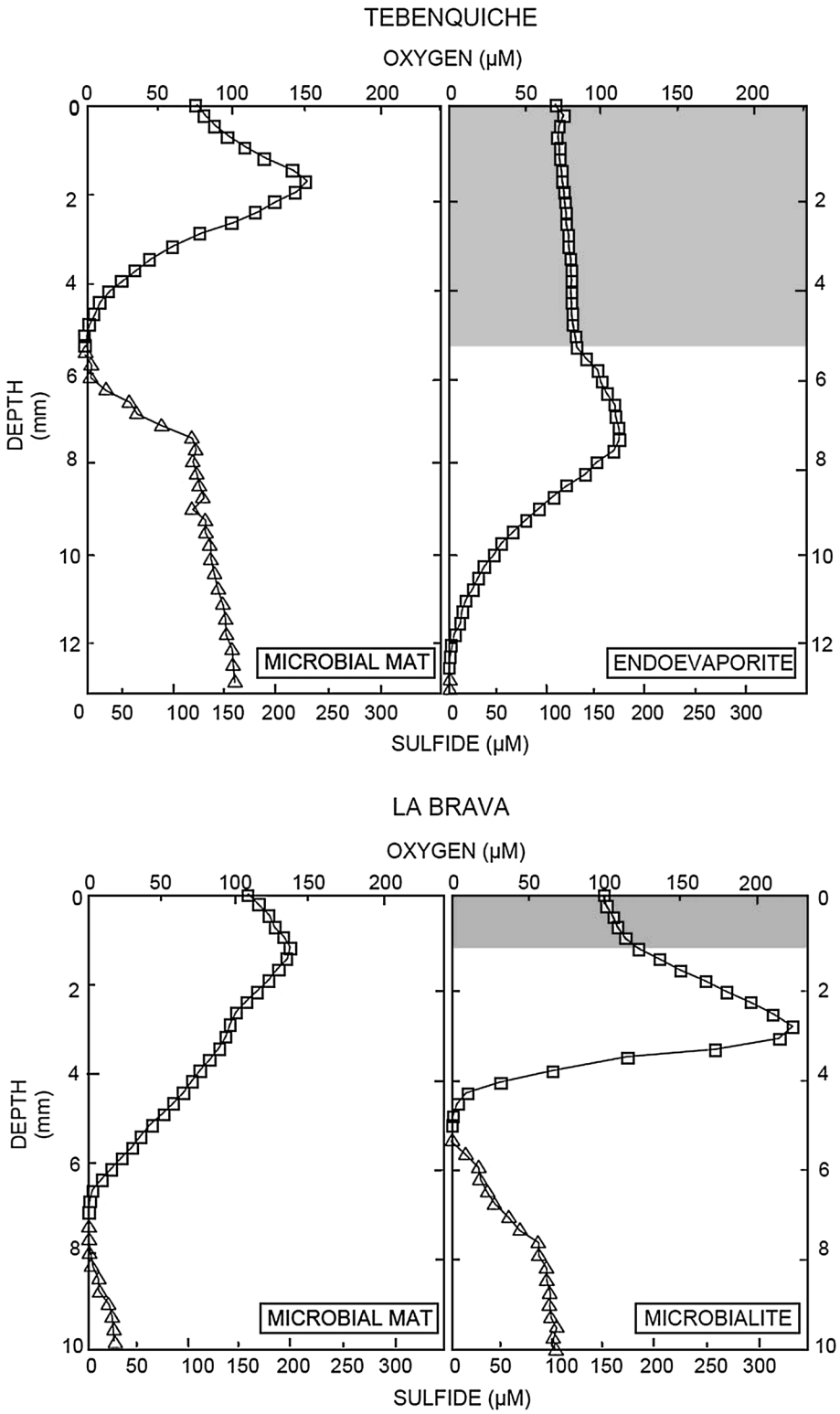

Fig. 5 Representative depth profiles of the concentration of O_2 (*squares*) and sulfide (*triangles*) measured in situ with microelectrodes during the light period. The *gray shaded* area depicts the mineral crust in the hard mats

Discussion

In this study is the first report of the presence of sedimentary microbial ecosystems (i.e., microbial mats, gypsum domes and carbonate microbialites) in Laguna Tebenquiche and La Brava. The dominant mineral in the microbial ecosystems of La Brava was aragonite, whereas in Tebenquiche, this was gypsum. Tebenquiche's calcium

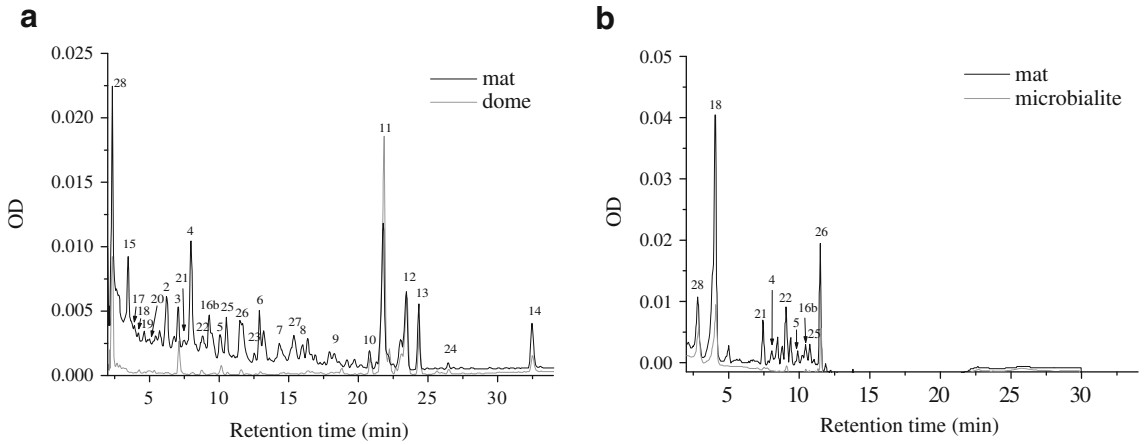

c

Pigment	Tebenquiche Mat (mg/L)	Tebenquiche Dome (mg/L)
Chlorophyll a	1.79	3.49
β-carotene	0.15	0.05
Lycopene	0.38	0.25
Diatoxanthin	0.26	0.05
Astaxanthin	0.15	ND

Fig. 6 Chromatogram of the methanol extract from microbial mats, microbialites and gypsum domes of Laguna Tebenquiche (**a**) and Laguna Brava (**b**) at 435 nm. The chromatograms of mat samples are represented by *black lines* and those of microbialites and the domes samples by *grey lines*. (**c**) Pigment concentrations in mat and dome samples of Laguna Tebenquiche (*ND* not detected)

sulfate brine is expected to generate mainly gypsum in agreement with Andean brines and wetlands like Atacama and Puquios (e.g., Salar de Llamara and Laguna de Piedra; Demergasso et al. 2003; Stivaletta et al. 2011). In contrast, La Brava's calcium carbonate brine, typical for the marginal zone of the Salar, could possibly support carbonate precipitation, and the elevated Mg concentration in this brine would favor precipitation of aragonite over calcite (see below). The lower salinity in La Brava compared to Tebenquiche could explain the precipitation of carbonates. More likely, the combination of the chemical composition of the brine and the high microbial activity in La Brava's sediments (Fig. 5) point to a possible microbially induced organomineralization, forming the $CaCO_3$ deposits (due to specific binding of Ca to EPS; Dupraz et al. 2009). This scenario is speculative, since an annual flow and water chemistry was not assessed in this study. Ongoing studies will help clarifying possible mechanisms of mineralization.

In Tebenquiche, the transition from non-lithifying mats (TM) to microbialite domes (TD) is coupled to an increase in salinity of the specific site water. The opposite scenario was found probably due to the input of ground water (Risacher et al. 2003) in La Brava, where the salinity of the overlying water decreased from BM to BMI. With increasing salinity, carbonates precipitate first, followed by sulfates and finally halite (Usiglio 1849). At low Mg concentrations, calcite precipitation is favored over that of aragonite (Flügel 2004). As a result, mineral precipitation in Salar de Atacama is not necessarily correlated with salinity, but with the actual chemical composition of the site water. Furthermore, the EPS, which is a major component of the mats, has been shown to tightly bind cations like Ca^{2+} and to a lesser extent Mg^{2+} (Decho 2000; Dupraz and Visscher 2005; Braissant et al. 2007, 2009). The specific binding capacity of the EPS may differ with different mat communities and varies with depth due to microbial activity (Braissant et al. 2009), both of which processes change the pore water chemistry of the mat. It is therefore conceivable that if the Ca-binding capacity is high, halite precipitation is not preceded by aragonite (or calcite) and/or gypsum precipitation. Alternatively, the removal of DIC (inorganic carbon) by carbon-fixing autotrophs could lower the carbonate concentration and as a result, lower the saturation index of calcium carbonate. This scenario would apply to a young (active) mat that is subject to evaporation. Finally, an alternative and a more plausible scenario for the presence of halite in the non-lithifying mat is the binding and trapping of this mineral. The trapping and binding capacity of sediment particles by organic-rich mats, which

Table 2 Pigments distribution in mat, dome and microbialite samples from Tebenquiche and La Brava

Retention time (min)	Peak	Related pigment	Tebenquiche		La Brava	
			Mat	Dome	Mat	Microbialite
2.85	28	390–(450)–(580)	–	–	0.204	0.142
3.47	17	330–410–550–610–670	0.365	–	–	–
3.55	15	Zeaxanthin	0.090	–	–	–
3.89	18	397–(465)–(500)–660	0.090	–	–	–
4.21	19	Echinenone	0.057	–	1.000	0.296
4.88	20	(400)–410–615	0.000	–	–	–
6.21	2	Diatoxanthin	0.142	–	–	–
7.03	3	Lycopene	0.073	0.048	–	–
7.78	21	325–(350)–410–615–660	0.057	–	0.012	–
7.90	4	435–465–(517)	0.170	–	0.057	–
8.83	22	Derivative of Lycopene	0.036	0.008	0.222	0.022
9.99	5	Aloxanthin	0.044	0.015	0.109	
10.49	16b	Bacteriochlorophyll *c*	0.062	–	0.110	–
10.54	25	430–476	0.081	–	0.107	–
11.52	26	Fucoxanthin	0.056	0.007	0.350	0.124
12.52	23	435–675	0.015	–	–	–
12.84	6	Astaxanthin	0.081	–	–	–
14.48	7	420–470	0.030	–	–	–
15.36	27	(390)–415–655	0.074	–	–	–
16.30	8	310–380–430–685	0.028	–	–	–
18.58	9	Bacteriochlorophyll *d*	0.021	–	–	–
20.73	10	407–650	0.031	0.029	–	–
21.68	11	Chlorophyll *a*	0.264	0.516	–	–
23.37	12	410–650	0.264	0.208	–	–
24.26	13	Bacteriochlorophyll *e*	0.106	0.090	–	–
26.45	24	Diadinoxanthin	0.009	0.008	–	–
32.43	14	β-carotene	0.084	0.029	–	–

Peak areas are provided as an indicator of relative pigmemt quantities; - indicates that no peak was observed

are characterized by copious amounts of EPS, has been well established (e.g., Dupraz and Visscher 2005; Dupraz et al. 2011).

Carbonate precipitation in mats involves an "alkalinity engine," (microbial community metabolism that generates carbonate alkalinity) and the presence of organic exopolymeric substances (EPS), which is not only important as a Ca-binding matrix but also as the site of mineral nucleation and growth. For example, oxygenic and anoxygenic photosynthesis and sulfate reduction promote carbonate precipitation, and aerobic respiration and sulfide oxidation support dissolution (Visscher et al. 1998; Dupraz and Visscher 2005). $CaCO_3$ crystals were present in microbial mats (Figs. 3b, 5) likely in close proximity to active sulfate reduction (e.g., the Deltaproteobacterial orders: Desulfovibrionales and *Syntrophobacter*), which could account for carbonate precipitation.

The microbial ecosystems found in the two lakes in the Atacama desert fall into three categories: non-lithifying mats found in La Brava (BM) and Tebenquiche (TM), lithifying platforms, or microbialites in La Brava made up of aragonite (BMI) and lithifying endoevaporitic systems in Tebenquiche that form domal structures that consist of gypsum (TD). This classification allows for comparisons with respect to Eubacterial diversity at two levels: between lakes (La Brava vs Tebenquiche) and between mat ecosystems non-lithifying mats vs. lithified (i.e., gypsum domes and aragonitic microbialites). It should be noted that this study did not include Archaeal diversity, and therefore, the results and conclusions present only a partial view of the systems that were investigated in this study.

All diversity metrics (Table 3) indicated that TM, BM and BMI displayed higher abundance, diversity and equitability than the TD. Previous results from microbial mats in salterns of Guerrero Negro, Mexico, also showed a vast biological complexity of these benthic ecosystems suggesting that positive feedback mechanisms exist between chemical complexity and biological diversity (Ley et al. 2006). In fact, the diversity in both environments of our study differs vastly when compared at the phylum level:

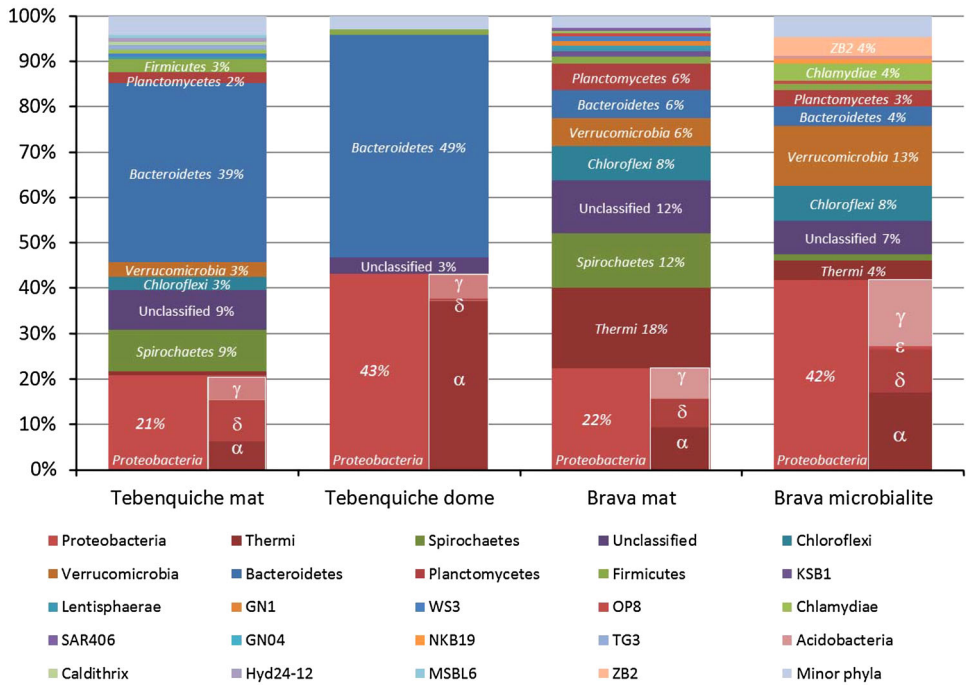

Fig. 7 Phylum-level abundance based on 16S rRNA sequence classification. *Vertical bars* reflect the percentage of 16S rRNA sequences assigned to each phylum using QIIME (Caporaso et al. 2010). Proteobacteria represent one of the major groups, particularly in the La Brava samples. Bacteroidetes are dominant in the Tebenquiche samples. Sequences that could not be assigned to any phylum (with a confidence threshold of 80 %) are labeled as "Unclassified". Approximately 15 phyla (depending on the sample) with contents <1 % are grouped as "Minor phyla"

Table 3 Diversity metrics for the sampled environments, using 16S rDNA V4 region sequences clustered at similarity level of 0.97 and normalized to 1500 sequences per sample

Ecosystem OTUs at 97 % similarity	CHAO1	Dominance	Equitability	Observed OTU	Shannon biodiversity index	Simpson index
Tebenquiche mat	592 (504/725)	0.037 (0.036/0.037)	0.795 (0.794/0.796)	335 (331/337)	6.668 (6.650/6.683)	0.963 (0.963/0.964)
Tebenquiche dome	242 (186/350)	0.162 (0.149/0.175)	0.580 (0.566/0.592)	129 (119/139)	4.065 (3.960/4.176)	0.838 (0.825/0.851)
Brava mat	527 (462/625)	0.031 (0.028/0.033)	0.815 (0.809/0.823)	337 (325/348)	6.841 (6.777/6.914)	0.969 (0.967/0.972)
Brava microbialite	614 (520/754)	0.032 (0.030/0.034)	0.787 (0.780/0.794)	331 (321/343)	6.591 (6.510/6.673)	0.984 (0.975/0.977)
Socompa (a)	710 (592/885)	0.023 (0.021/0.025)	0.805 (0.793/0.814)	348 (328/368)	6.797 (6.685/6.922)	0.977 (0.975/0.977)

Confidence intervals at 95 % are shown in parenthesis. Data from Socompa stromatolite (SRA accession number SRA061755, (Farías et al. 2013)) are shown for comparison

Thermi (Deinococci), Verrucomicrobia (Spartobacteria) presented relatively high abundance in carbonate systems (i.e., La Brava), but were virtually absent in the gypsum domes (Tebenquiche). In contrast, Bacteroidetes were dominant in Tebenquiche's endoevaporites and underrepresented in the carbonate deposits of La Brava. Similar results were observed in other Andean microbialite systems: in Socompa stromatolites, which form through microbial aragonite precipitation, Deinococci were relatively well represented (7 %), but Bacteroidetes were almost undetected (1 %) (Farías et al. 2013).

As mentioned above, Deinococcus-Thermus was much more abundant in La Brava than in Tebenquiche (BM 18 % and BMI 4 %, and <1 % in TM and TD). A possible explanation for this observation is that in mats (BM) and the aragonite microbialites (BMI), the bacterial communities are more exposed to UV than in gypsum domes: UV is quenched by the gypsum crust and exposure to endoevaporitic communities minimized. The gypsum domes are a refuge for the endoevaporitic communities by offering protection against excessive radiation as well as desiccation (Oren et al. 1995). High abundance of *Deinococcus* was also reported in several high-altitude microbial systems found in Obsidian Pool siliceous mats at 2,400 m asl in Yellowstone NP, and in the pink upper layer of Socompa stromatolites at 3,600 m asl in the Argentinean Andes (Farías et al. 2013). The carotenoid deinoxanthin of *Deinococcus* would give Socompa microbialites and BM their pink appearance. This phylum is generally a minor contributor to diversity in low-altitude microbialites (Baumgartner et al. 2009a, b; Mobberley et al. 2012). Based on these observations, we hypothesize that *Deinococcus* proliferates at high altitude, which provides a selective advantage to outcompete other microorganisms in a high-UV

irradiance, anoxic and organic-rich environment (i.e., the mat surface), and that their pigmentation provides protection from UV light for the other members of the mat community.

In contrast to *Deinococcus*, the phylum Bacteroidetes dominated Tebenquiche gypsum domes (49 % of total sequences) and microbial mats (39 % of total sequences), but was virtually absent in the La Brava systems (6 % in BM and 4 % in BMI). This phylogenetic group is commonly observed in aquatic environments and sediments, including fresh and marine waters (Bowman et al. 2000; Kirchman 2002; Humayoun et al. 2003). Bacteroidetes are a dominant phylum in hypersaline systems, including microbial mats (Ley et al. 2006; Green et al. 2008) and microbialites (Baumgartner et al. 2009b; Visscher et al. 2010). Similarly, Bacteroidetes were a dominant group in both water and sediment samples of high-altitude hypersaline lakes from the Andes and the Tibetan Plateau (Demergasso et al. 2004, 2008, 2010; Dorador 2007; Jiang et al. 2007). In a shallow, hypersaline lake in Eleuthera, Bahamas, non-lithifying and lithifying mats along a transect generally showed a 6–10 times higher contribution of Bacteroidetes in the lithifying systems (Baumgartner et al. 2009b). This trend of increased contribution to total diversity in lithifying systems is similar to our observation for Tebenquiche mats and endoevaporites. A predominance of Bacteroidetes was also reported in (endo)evaporitic gypsum domes from the Llamara lagoon in Salar de Puquios (unpublished). It appears that Bacteroidetes increase their presence with increasing salinity and possibly are also associated with gypsum (endo)evaporites but not with calcium carbonate microbialites.

Spartobacteria, a subphylum of Verrucomicrobia, were well represented in mainly in BMI (13 %) but also were present in mats (6 % BM–3 % TM). This bacterial group is typically found in soil or associated with nematodes

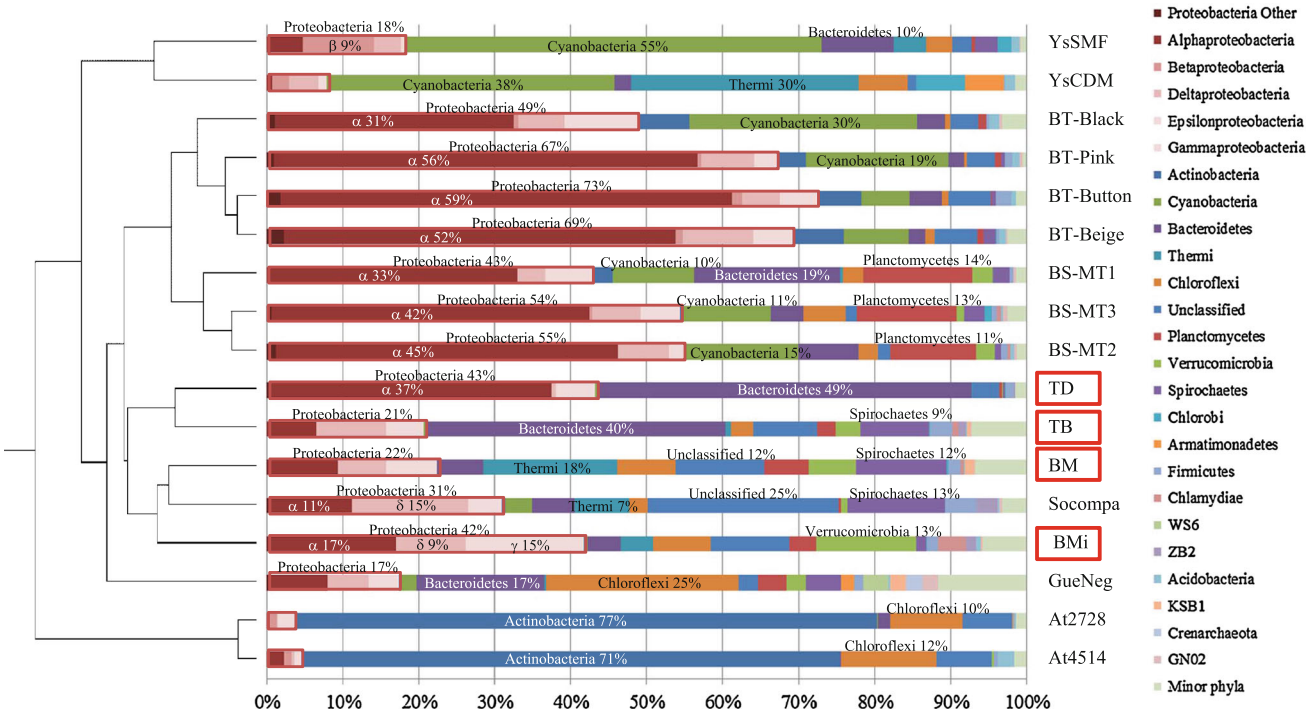

Fig. 8 Phylum-level abundance based on 16S rRNA sequence classification using QIIME (Caporaso et al. 2010). Sequences that could not be assigned to any phylum (with a confidence threshold of 80 %) are depicted as "Unclassified". Approximately 15 phyla (depending on the sample) with contents <2 % are grouped as "Minor phyla". Different mats and microbialites of this study (Laguna Tebenquiche: TD, Tebenquiche dome; TM, Tebenquiche mat) and Laguna Brava (*BMI* Brava microbialite, *BM* Brava mat. SRA061755, this study) were compared to other microbial mat and microbialite systems: Socompa stromatolite (Socompa. SRA accession number SRP007748; Farías et al. 2013), Atacama hyper-arid soils (At2728 and At4514. SRA030747; Neilson et al. 2012), Yellowstone stromatolites (*YsCDM* exposed stromatolite, *YsSMF* submerged stromatolite) Pepe-Ranney et al. 2012), Highborne Cay stromatolites, Bahamas (BS-MT1. BS-MT2. BS-MT3. GenBank accession numbers FJ911975–FJ912833; Baumgartner et al. 2009a), Highborne Cay thrombolites, Bahamas (BT-Black. BT-Pink. BT-Button. BT-Beige. SRX030166; Mobberley et al. 2012), and the Guerrero Negro microbial mat, Mexico (GueNeg. GenBank accession numbers DQ329539 to DQ331020 and DQ397339 to DQ397511; Ley et al. 2006). The analyses were done on subsampled datasets containing 224 sequences (corresponding to Bahamas stromatolite samples, the smallest dataset). Similarities of the compared microbial mat communities were derived from the Bray Curtis metric calculated at phylum level. Similar results were obtained using 980 sequences and omitting Bahamas stromatolite samples from the analysis

which are commonly found in mats (Baumgartner et al. 2009a, b; Ley et al. 2006), but were also abundant around fumaroles at Socompa, (Costello et al. 2009) an active volcano (6,051 m asl) near our field site and in alkaline, mesophilic microbial mats in Romania (Coman et al. 2013).

Despite some marked differences, Tebenquiche and La Brava diversities are more similar to each other than to other microbial mat and microbialites including those found in open marine, hypersaline and hydrothermal environments (Fig. 8), with the exception of the nearby Socompa stromatolites. It is not surprising that the extreme physicochemical and geochemical conditions characteristic for the High Altitude Andean ecosystems would support the growth of similar microbial phyla, which differ from phyla found in stromatolites and thrombolites at sea level (Baumgartner et al. 2009a; Mobberley et al. 2012, Farías et al. 2013). Further comparison shows that the Tebenquiche and La Brava microbialites diversities are more similar to that of the aragonitic open marine Bahamian stromatolites and thrombolites (Reid et al. 2000; Myshrall et al. 2010) than to that of the hypersaline, siliciclastic mats of Guerrero Negro, Mexico (Ley et al. 2006). This suggests that a correlation between mineral composition and diversity might exist or, alternatively, that the salinity controlling which mineral precipitates determines the microbial diversity of a given system.

Gypsum domes are found in association with (endo)evaporites comprised of diverse communities that include diatoms, cyanobacteria and purple sulfur bacteria arranged along opposing gradients of light and hydrogen sulfide. EPS produced by various microorganisms, notably cyanobacteria, could act as site for selenite (a variety of gypsum) nucleation, forming the nucleation site for gypsum precipitation similar to that observed for carbonate precipitation (Fig. 3e, g, h). SRB are capable of dissolving gypsum when using sulfate for respiration (Ollivier et al. 1994) and sulfide-oxidizers (chemolithotrophic and phototrophic) can precipitate gypsum (Kelly and Harrison 1989; Petrash et al. 2012). Petrash et al. 2012 proposed a six-step formation mechanism of $CaCO_3$- and $CaSO_4$-containing thrombolites in Venezuela. According to their model, either gypsum or calcium carbonate will be the predominant mineral product, depending on the composition of the microbial community and the water chemistry (e.g., $[Mg^{2+}]$ concentration). Layered (i.e., microbial mat) communities exist within gypsum crusts at numerous locations: France (Caumette 1993; Caumette et al. 1994), Italy (Margheri et al. 1987), Egypt (Taher et al. 1995; Ali-Bik et al. 2011), Israel (Oren et al. 2009), Mexico (Spear et al. 2003; Vogel et al. 2010), Venezuela (Petrash et al. 2010) and at various other hypersaline sites (Rothschild et al. 1994; Airs and Keely 2003). Furthermore, gypsum-containing microbialites frequently occur in the fossil record (Peryt 1996; Peryt et al. 2004), and possibly exist on Mars (Gendrin et al. 2005; Vogel et al. 2009).

Acknowledgments This work was supported by Préstamo BID PICT 2010 No. 1788-Agencia Nacional de Promoción Científica y Tecnológica and Loreal-CONICET-UNESCO for Women in Science price. Flores, Kurth, Rasuk and Maldonado are recipients of a CONICET fellowship. We also want to thank Lic. Cecilia Genazzini and Mr. Pablo García of CONICET for their assistance in the XRD laboratory.

References

Airs RL, Keely BJ (2003) A high resolution study of the chlorophyll and bacteriochlorophyll pigment distributions in a calcite/gypsum microbial mat. Org Geochem 34:539–551

Ali-Bik MW, Metwally HI, Kamel MG, Wali AM (2011) Gypsum and dolomite biomineralization in endoevaporitic microbial niche, EMISAL, Fayium, Egypt. Environ Earth Sci 62:151–159

Alonso H, Risacher F (1996) Geoquímica del Salar de Atacama, parte 1: origen de los componentes y balance salino. Andean Geol 23:113–122

Arp G, Thiel V, Reimer A, Michaelis W, Reitner J (1999a) Biofilm exopolymers control microbialite formation at thermal springs discharging into the alkaline Pyramid Lake, Nevada, USA. Sediment Geol 126:159–176

Arp G, Reimer A, Reitner J (1999b) Calcification in cyanobacterial biofilms of alkaline salt lakes. Eur J Phycol 34:393–403

Babel M (2004) Models for evaporite, selenite and gypsum microbialite deposition in ancient saline basins. Acta Geol Pol 54:219–249

Baumgartner LK, Spear JR, Buckley DH, Pace NR, Reid RP, Dupraz C, Visscher PT (2009a) Microbial diversity in modern marine stromatolites, Highborne Cay, Bahamas. Environ Microbiol 11:2710–2719

Baumgartner LK, Dupraz C, Buckley DH, Spear JR, Pace NR, Visscher PT (2009b) Microbial species richness and metabolic activities in hypersaline microbial mats: insight into biosignature formation through lithification. Astrobiology 9:861–874

Bevacqua P (1992) Geomorfología del salar de Atacama y estratigrafía de su núcleo y delta, Segunda Región de Antofagasta, Chile. Memoria de Título (Inédito), Universidad Católica del Norte, Facultad de Ingeniería y Ciencias Geólogicas, 284 p. Antofagasta

Beveridge TJ (1981) Ultrastructure, chemistry, and function of the bacterial wall. Int Rev Cytol 72:229–317

Borrego CM, Garcia-Gil LJ (1994) Separation of bacteriochlorophyll homologues from green photosynthetic bacteria by reversed-phase HPLC. Photosynth Res 41:157–163

Bowman JP, Rea SM, McCammon SA, McMeekin TA (2000) Diversity and community structure within anoxic sediment from marine salinity meromictic lakes and a coastal meromictic marine basin, Vestfold Hills, Eastern Antarctica. Environ Microbiol 2:227–237

Braissant O, Cailleau G, Aragno M, Verrecchia EP (2004) Biologically induced mineralization in the tree *Milicia excelsa* (Moraceae): its causes and consequences to the environment. Geobiology 2:59–66

Braissant O, Decho AW, Dupraz C, Glunk C, Przekop KM, Visscher PT (2007) Exopolymeric substances of sulfate-reducing bacteria: interactions with calcium at alkaline pH and implication for formation of carbonate minerals. Geobiology 5:401–411

Braissant O, Decho AW, Przekop KM, Gallagher KL, Glunk C, Dupraz C, Visscher PT (2009) Characteristics and turnover of exopolymeric substances in a hypersaline microbial mat. FEMS Microbiol Ecol 67:293–307

Burne RV, Moore LS (1987) Microbialites: organosedimentary deposits of benthic microbial communities. Palaios 2:241–254

Cabrera S, Pizarro G (1994) Changes in chlorophyll *a* concentration, copepod abundance and UV and PAR penetration in the water column during the ozone depletion in Antarctic Lake Kitiesh, 1992. Adv Limnol/Ergeb Limnol 43:123–134

Canfield DE, Sorensen KB, Oren A (2004) Biogeochemistry of a gypsum-encrusted microbial ecosystem. Geobiology 2:133–150

Caporaso JG, Kuczynski J, Stombaugh J, Bittinger K, Bushman FD, Costello EK, Fierer N, Gonzalez Peña A, Goodrich AK, Gordon JI, Huttley GA, Kelley ST, Knights D, Koenig JE, Ley RE, Lozupone CA, McDonald D, Muegge BD, Pirrung M, Reeder J, Sevinsky JR, Turnbaugh PJ, Walters WA, Widmann J, Yatsunenko T, Zaneveld J, Knight R (2010) QIIME allows analysis of high-throughput community sequencing data. Nat Methods 7:335–336

Caumette P (1993) Ecology and physiology of phototrophic bacteria and sulfate-reducing bacteria in marine salterns. Experientia 49:473–481

Caumette P, Matheron R, Raymond N, Relexans J (1994) Microbial mats in the hypersaline ponds of Mediterranean salterns (Salins-de-Giraud, France). FEMS Microbiol Ecol 13:273–286

Cody AM, Cody RD (1989) Evidence for microbiological induction of [101] montmartre twinning of gypsum ($CaSO_4{\cdot}2H_2O$). J Cryst Growth 98:721–730

Coman C, Drugă B, Hegedus A, Sicora C, Dragoş N (2013) Archaeal and bacterial diversity in two hot spring microbial mats from a geothermal region in Romania. Extremophiles 17:523–534

Costello EK, Halloy SR, Reed SC, Sowell P, Schmidt SK (2009) Fumarole-supported islands of biodiversity within a hyperarid, high-elevation landscape on Socompa Volcano, Puna de Atacama, Andes. Appl Environ Microbiol 75:735–747

Decho AW (2000) Exopolymer microdomains as a structuring agent for heterogeneity within microbial biofilms. In: Riding RE, Awramik SM (eds) Microbial sediments. Springer, Berlin, pp 9–15

Demergasso C, Chong G, Galleguillos P, Escudero L, Martinez-Alonso M, Steve I (2003) Microbial mats from the Llamara salt flat, northern Chile. Rev Chil Hist Nat 76:485–499

Demergasso C, Casamayor EO, Chong G, Galleguillos P, Escudero L, Pedròs-Aliò C (2004) Distribution of prokaryotic genetic diversity in athalassohaline lakes of the Atacama Desert, Northern Chile. FEMS Microbiol Ecol 48:57–69

Demergasso C, Escudero L, Casamayor EO, Chong G, Balague V, Pedros-Alió C (2008) Novelty and spatio-temporal heterogeneity in the bacterial diversity of hypersaline Lake Tebenquiche (Salar de Atacama). Extremophiles 12:491–504

Demergasso C, Dorador C, Meneses D, Blamey J, Cabrol N, Escudero L, Chong G (2010) Prokaryotic diversity pattern in high-altitude ecosystems of the Chilean Altiplano. J Geophys Res 115:G00D09

Dorador C (2007) Microbial communities in high altitude altiplanic wetlands in northern Chile: phytogeny, diversity and function. Doctoral dissertation, Christian-Albrechts-Universität, Kiel, Germany, p 166

Dorador C, Meneses D, Urtuvia V, Demergasso C, Vila I, Witzel KP, Imhoff JF (2009) Diversity of *Bacteroidetes* in high-altitude saline evaporitic basins in northern Chile. J Geophys Res 114:G00D05

Douglas S (2005) Mineralogical footprints of microbial life. Am J Sci 305:503–525

Dupraz C, Reid RP, Visscher PT (2011) Modern microbialites. In: Reitner J, Thiel V (eds) Encylopedia of geobiology. Springer, Berlin, pp 617–634

Dupraz C, Visscher PT (2005) Microbial lithification in marine stromatolites and hypersaline mats. Trends Microbiol 13:429–438

Dupraz C, Visscher PT, Baumgartner LK, Reid RP (2004) Microbe–mineral interactions: early carbonate precipitation in a hypersaline lake (Eleuthera Island, Bahamas). Sedimentology 51:745–765

Dupraz C, Reid RP, Braissant O, Decho AW, Norman RS, Visscher PT (2009) Processes of carbonate precipitation in modern microbial mats. Earth Sci Rev 96:141–162

Eaton AD, Clesceri LS, Rice EW, Greenberg AE, Franson MAH (2005) Standard methods for the examination of water and wastewater: Centennial edition. American Public Health Association, Washington DC, p 1368

Farías ME, Rascovan N, Toneatti DM, Albarracín VH, Flores MR, Poiré DG, Collavino MM, Aguilar OM, Vázquez MP, Polerecky L (2013) The discovery of stromatolites developing at 3570 m above sea level in a high-altitude volcanic lake Socompa, Argentinean Andes. PloS One 8:e53497

Flügel E (2004) Microfacies of carbonate rocks. Springer, Berlin

Gallagher KL, Braissant O, Kading TJ, Dupraz C, Visscher PT (2010) Phosphate-related artifacts in carbonate mineralization experiments. J Sediment Res 83:37–49

Gendrin A, Mangold N, Bibring J-P, Langevin Y, Gondet B, Poulet F, Bonello G, Quantin C, Mustard J, Arvidson R, LeMouélic S (2005) Sulfates in martian layered terrains: the OMEGA/Mars express view. Science 307:1587–1591

Gerdes G (2007) Structures left by modern microbial mats in their host sediments. In: Schieber J, Bose PK, Eriksson PG, Banerjee S, Sarkar S, Altermann W, Catuneau O (eds) Atlas of microbial mat features preserved within the clastic rock record. Elsevier, Amsterdam, pp 5–38

Gerdes G, Dunajtschik-Piewak K, Riege H, Taher AG, Krumbein WE, Reineck HE (1994) Structural diversity of biogenic carbonate particles in microbial mats. Sedimentology 41:1273–1294

Glunk C, Dupraz C, Braissant O, Gallagher KL, Verrecchia EP, Visscher PT (2011) Microbially mediated carbonate precipitation in a hypersaline lake, Big Pond (Eleuthera, Bahamas). Sedimentology 58:720–736

Green SJ, Blackford C, Bucki P, Jahnke LL, Prufert-Bebout L (2008) A salinity and sulfate manipulation of hypersaline microbial mats reveals stasis in the cyanobacterial community structure. ISME J 2:457–470

Hounslow A (1995) Water quality data: analysis and interpretation. CRC Press, New York

Humayoun SB, Bano N, Hollibaugh JT (2003) Depth distribution of microbial diversity in Mono Lake, a meromictic soda lake in California. Appl Environ Microb 69:1030–1042

Jahnert RJ, Collins LB (2011) Significance of subtidal microbial deposits in Shark Bay, Australia. Mar Geol 286:106–111

Jahnert RJ, Collins LB (2013) Controls on microbial activity and tidal flat evolution in Shark Bay, Western Australia. Sedimentology 60:1071–1099

Jiang H, Dong H, Yu B, Liu X, Li Y, Ji S, Zhang CL (2007) Microbial response to salinity change in Lake Chaka, a hypersaline lake on Tibetan plateau. Environ Microbiol 9:2603–2621

Kelly DP, Harrison AP (1989) Aerobic chemolithotrophic bacteria and associated organisms. In: Hensyl WR et al (ed) Bergey's manual of systematic bacteriology, Vol 3. Williams and Wilkins, Baltimore, pp 1842–1858

Kirchman DL (2002) The ecology of *Cytophaga–Flavobacteria* in aquatic environments. FEMS Microbiol Ecol 39:91–100

Knoll AH, Golubic S (1992) Proterozoic and living cyanobacteria. In: Schidlowski M, Golubic S, Kimberley MM, McKirdy DM, Trudinger A (eds) Early organic evolution. Springer, Berlin, pp 450–462

Lara J, González LE, Ferrero M, Díaz GC, Pedrós-Alió C, Demergasso C (2012) Enrichment of arsenic transforming and resistant heterotrophic bacteria from sediments of two salt lakes in Northern Chile. Extremophiles 16:523–538

Ley RE, Harris JK, Wilcox J, Spear JR, Miller SR, Bebout BM, Maresca JA, Bryant DA, Sogin ML, Pace NR (2006) Unexpected diversity and complexity of the Guerrero Negro hypersaline microbial mat. Appl Environ Microb 72:3685–3695

López-López A, Yarza P, Richter M, Suárez-Suárez A, Antón J, Niemann H, Rosselló-Móra R (2010) Extremely halophilic microbial communities in anaerobic sediments from a solar saltern. Environ Microbiol Rep 2:258–271

Ludwig R (2004) Carbon cycling and calcification in hypersaline microbial mats. PhD dissertation, Biology/Chemistry, University of Bremen, Germany, p 157

Margheri MC, Tredici MR, Barsanti L, Balloni W (1987) The photosynthetic community of the Trapani saline lagoons: an alternative option for the exploitation of an extreme environment. Ann Microbiol 37:203–215

Mobberley JM, Ortega MC, Foster JS (2012) Comparative microbial diversity analyses of modern marine thrombolitic mats by barcoded pyrosequencing. Environ Microbiol 14:82–100

Myshrall KL, Mobberley JM, Green SJ, Visscher PT, Havemann SA, Reid RP, Foster JS (2010) Biogeochemical cycling and microbial diversity in the thrombolytic microbialites of Highborne Cay, Bahamas. Geobiology 8:337–354

Neilson JW, Quade J, Ortiz M, Nelson WM, Legatzki A, Tian F, LaComb M, Betancourt JL, Wing RA, Soderlund CA, Maier RM (2012) Life at the hyperarid margin: novel bacterial diversity in arid soils of the Atacama Desert, Chile. Extremophiles 16:553–566

Ollivier B, Caumette P, Garcia JL, Mah RA (1994) Anaerobic bacteria from hypersaline environments. Microbiol Rev 58:27–38

Oren A, Kuhl M, Karsten U (1995) An endoevaporitic microbial mat within a gypsum crust: zonation of phototrophs, photopigments, and light penetration. Mar Ecol Prog Ser 128:151–159

Oren A, Sørensen KB, Canfield DE, Teske AP, Ionescu D, Lipski A, Karlheinz A (2009) Microbial communities and processes within a hypersaline gypsum crust in a saltern evaporation pond (Eilat, Israel). Hydrobiology 626:15–26

Paterson DM (1994) Microbiological mediation of sediment structure and behaviour. In: Stal LJ, Caumette P (eds) Microbial mats. Springer, Berlin, pp 97–109

Pepe-Ranney C, Berelson WM, Corsetti FA, Treants M, Spear JR (2012) Cyanobacterial construction of hot spring siliceous stromatolites in Yellowstone National Park. Environ Microbiol 14:1182–1197

Peryt TM (1996) Sedimentology of Badenian (middle Miocene) gypsum in eastern Galicia, Podolia and Bukovina (West Ukraine). Sedimentology 43:571–588

Peryt TM, Peryt D, Jasionowski M, Poberezhskyy AV, Durakiewicz T (2004) Post-evaporitic restricted deposition in the Middle Miocene Chokrakian-Karaganian of East Crimea (Ukraine). Sediment Geol 170:21–36

Petrash DA, Lalonde SV, Pecoits E, Gingras MK, Konhauser KO (2010) Microbially-catalyzed cementation of modern gypsum-dominated thrombolites. Geochimica et Cosmochimica Acta 74:a811

Petrash DA, Gingras MK, Lalonde SV, Orange F, Pecoits E, Konhauser KO (2012) Dynamic controls on accretion and lithification of modern gypsum-dominated thrombolites, Los Roques, Venezuela. Sediment Geol 245–246:29–47

Reid RP, Visscher PT, Decho AW, Stolz JF, Bebout BM, Dupraz C, Macintyre IG, Paerl HW, Pinckney JL, Prufert-Bebout L, Steppe TF, DesMarais DJ (2000) The role of microbes in accretion, lamination and early lithification of modern marine stromatolites. Nature 406:989–992

Reid EA, Reid JS, Meier MM, Dunlap MR, Cliff SS, Broumas AA, Perry K, Maring H (2003) Characterization of African dust transported to puerto rico by individual particle and size segregated bulk analysis. J Geophys Res 108:16

Reitner J, Peckmann J, Blumenberg M, Michaelis W, Reimer A, Thiel V (2005) Concretionary methane-seep carbonates and associated microbial communities in Black Sea sediments. Palaeogeogr Palaeocl 227:18–30

Riding R (2011) Microbialites, stromatolites and thrombolites. In: Reitner J, Thiel V (eds) Encyclopedia of geology. Encyclopedia of earth science series. Springer, Heidelberg, pp 635–654

Risacher F, Alonso H, Salazar C (2003) The origin of brines and salts in Chilean salars: a hydrochemical review. Earth Sci Rev 63:249–293

Rothschild LJ, Giver LJ, White MR, Mancinelli RL (1994) Metabolic activity of microorganisms in evaporites. J Appl Phycol 30:431–438

Sahl JW, Pace NR, Spear JR (2008) Comparative molecular analysis of endoevaporitic microbial communities. Appl Environ Microb 74:6444–6446

Sanz Montero ME, Rodríguez Aranda JP (2008) Participación microbiana en la formación de magnesita dentro de un ambiente lacustre evaporítico: Mioceno de la Cuenca de Madrid. Macla 9:231–232

Sherwood JE, Stagnitti F, Kokkinn MJ, Williams WD (1991) Dissolved oxygen concentrations in hypersaline waters. Limnol Oceanogr 36:235–250

Spear JR, Ley RE, Berger AB, Pace NR (2003) Complexity in natural microbial ecosystems: the Guerrero Negro experience. Biol Bull 204:168–173

Stivaletta N, Barbieri R (2009) Endolithic microorganisms from spring mound evaporite deposits (southern Tunisia). J Arid Environ 73:33–39

Stivaletta N, López-García P, Boihem L, Millie DF, Barbieri R (2010) Biomarkers of endolithic communities within gypsum crusts (southern Tunisia). Geomicrobiol J 27:101–110

Stivaletta N, Barbieri R, Ceveninia F, López García P (2011) Physicochemical conditions and microbial diversity associated with the evaporite deposits in the Laguna de la Piedra (Salar de Atacama, Chile). Geomicrobiol J 28:83–95

Stoertz GE, Ericksen GE (1974) Geology of salars in northern Chile. US Geol Survey Professional Paper, vol 811, pp 65

Taher AG, Wahab SA, Philip G, Krumbein WE, Wali AM (1995) Evaporitic sedimentation and microbial mats in a salina system (Port Fouad, Egypt). Int J Salt Lake Res 4:95–116

Thompson JB, Ferris FG (1990) Cyanobacterial precipitation of gypsum, calcite, and magnesite from natural alkaline lake water. Geology 18:995–998

Usiglio J (1849) Analyse de I'eau de la Méditerranée sur les côtes de France. Ann Chemie 27:172–191

Vasconcelos C, McKenzie JA (1997) Microbial mediation of modern dolomite precipitation and diagenesis under anoxic conditions (Lagoa Vermelha, Rio de Janeiro, Brazil). J Sediment Res 67:378–390

Visscher PT, Stolz J (2005) Microbial mats as: populations, process and products reactors. Palaeogeogr Palaeocl 219:87–100

Visscher PT, Reid RP, Bebout BM, Hoeft SE, Macintyre IG, Thompson JA (1998) Formation of lithified micritic laminae in

modern marine stromatolites (Bahamas): the role of sulfur cycling. Am Mineral 83:1482–1493

Visscher PT, Dupraz C, Braissant O, Gallagher KL, Glunk C, Casillas L, Reed RE (2010) Biogeochemistry of carbon cycling in hypersaline mats: linking the present to the past through biosignatures. In: Seckbach J, Oren A (eds) Microbial mats. Springer, Netherlands, pp 443–468

Vogel MB, Des Marais DJ, Turk KA, Parenteau MN, Jahnke LL, Kubo MD (2009) The role of biofilms in the sedimentology of actively forming gypsum deposits at Guerrero Negro, Mexico. Astrobiology 9:875–893

Vogel MB, Des Marais DJ, Parenteau MN, Jahnke LL, Turk KA, Kubo MD (2010) Biological influences on modern sulfates: textures and composition of gypsum deposits from Guerrero Negro, Baja California Sur, Mexico. Sediment Geol 223:265–280